International Journal of Computational Intelligence Systems (2023) 16:129
https://doi.org/10.1007/s44196-023-00304-8

RESEARCH ARTICLE

Revolutionizing Vehicle Cruise Control: An Elite Opposition-Based Pattern Search Mechanism Augmented INFO Algorithm for Enhanced Controller Design

Serdar Ekinci[1] · Davut Izci[1,2] · Laith Abualigah[3,7,8,9] · Abdelazim G. Hussien[4,5] · Cuong-Le Thanh[3] · Samir Khatir[3,6]

Received: 26 April 2023 / Accepted: 21 July 2023
© The Author(s) 2023

Abstract
This paper presents a groundbreaking approach to enhance the performance of a vehicle cruise control system—a crucial aspect of road safety. The work offers two key contributions. Firstly, a state-of-the-art metaheuristic algorithm is proposed by augmenting the performance of the weighted mean of vectors (INFO) algorithm using pattern search and elite opposition-based learning mechanisms. The resulting boosted INFO (b-INFO) algorithm surpasses the original INFO, marine predators, and gravitational search algorithms in terms of performance on benchmark functions, including unimodal, multimodal, and fixed-dimensional multimodal functions. Secondly, a novel proportional, fractional order integral, derivative plus double derivative with filter ($PI^{\lambda}DND^2N^2$) controller is proposed as a more efficient control structure for vehicle cruise control systems. An objective function is utilized to determine the optimal values for the controller parameters, and the proposed method's performance is compared against a range of recent approaches. Results demonstrate that the b-INFO algorithm-based $PI^{\lambda}DND^2N^2$ controller is the most efficient and superior method for controlling a vehicle cruise control system. Moreover, this work represents the first report of a $PI^{\lambda}DND^2N^2$ controller's implementation for vehicle cruise control systems, underscoring the novelty and significance of this research. The proposed method's exceptional ability is further confirmed by comparisons with the genetic algorithm, ant lion optimizer, atom search optimizer, arithmetic optimization algorithm, slime mold algorithm, Lévy flight distribution algorithm, manta ray foraging optimization, and hunger games search-based proportional–integral–derivative (PID), along with Harris hawks optimization-based PID and fractional order PID controllers. This work marks a remarkable milestone toward safer and more efficient vehicle cruise control systems.

Keywords Vehicle cruise control system · Pattern search · Elite opposition-based learning · Weighted mean of vectors algorithm

✉ Laith Abualigah
aligah.2020@gmail.com

✉ Abdelazim G. Hussien
aga08@fayoum.edu.eg; abdelazim.hussien@liu.se

[1] Department of Computer Engineering, Batman University, 72100 Batman, Turkey

[2] MEU Research Unit, Middle East University, Amman, Jordan

[3] Center for Engineering Application and Technology Solutions, Ho Chi Minh City Open University, Ho Chi Minh 700000, Vietnam

[4] Department of Computer and Information Science, Linköping University, Linköping, Sweden

[5] Faculty of Science, Fayoum University, Fayoum, Egypt

[6] Laboratory Soete, Department of Electrical Energy, Metals, Mechanical Constructions, and Systems, Faculty of Engineering and Architecture, Ghent University, 9000 Ghent, Belgium

[7] Hourani Center for Applied Scientific Research, Al-Ahliyya Amman University, Amman 19328, Amman, Jordan

[8] Department of Electrical and Computer Engineering, Lebanese American University, Byblos 13-5053, Lebanon

[9] Applied science research center, Applied science private university, Amman 11931, Amman, Jordan

Published online: 08 August 2023

1 Introduction

Nowadays, drivers are eager to have their vehicles integrated with vehicle cruise control systems, as such mechanisms provide comfort in long journeys and significantly reduce driver-related accidents [1]. Not only does the safety factor come into play, but there is also a considerable reduction in fuel consumption, making the cruise control system a vital requirement for consumers [2]. However, a convenient control mechanism is crucial for operating such a system with the desired efficiency [3]. Therefore, in the previously reported works, the use of different controller mechanisms such as proportional–integral–derivative (PID) [4], PID with reference model [5], fractional-order PID (FOPID) [6], real PID plus second-order derivative ($PIDD^2$) [7], fuzzy logic [8], adaptive [9] and model predictive [10] controllers can be encountered for operation of vehicle cruise control systems.

Despite the existence of those mechanisms, there is still room for newer controllers for reaching more excellent performance characteristics [7]. The latter is an important challenge that needs attention. In this regard, this paper proposes proportional, fractional order integral, derivative plus double derivative with filter ($PI^{\lambda}DND^2N^2$) controller [11] as a new and more efficient solution for a vehicle cruise control system compared to PID and FOPID controllers. The reason of the proposal of $PI^{\lambda}DND^2N^2$ controller is due to its efficiency in reducing the overshoot, settling and rise time of the system [12]. Moreover, the $PI^{\lambda}DND^2N^2$ controller has two additional low pass filters which let the derivative terms to reduce the high frequency gain and noise appropriately [11]. It is also worth noting that this paper is also the first report demonstrating the implementation of a $PI^{\lambda}DND^2N^2$ controller for efficient operation of a vehicle cruise control system.

The proposed $PI^{\lambda}DND^2N^2$ controller has seven parameters (K_P, K_I, K_D, K_{DD}, λ, N_1 and N_2) which require to be adjusted similar to the case for PID [13] and FOPID [14] controllers. Therefore, an efficient adjustment method is also required to tune those parameters to optimal values. In terms of tuning such parameters, metaheuristic algorithms have been demonstrated as the most convenient options in the reported works [15]. With regards to vehicle cruise control system, enhanced reptile search algorithm [16], ant lion optimization algorithm [5], differential evolution algorithm [17], atom search optimization algorithm [18], genetic algorithm [19], hunger games search algorithm [20], arithmetic optimization algorithm [21] and Harris hawks optimization algorithm [22] can be found as the recent metaheuristic approaches for adjustment of different controllers.

The examples mentioned above, and the reported good results were considered in this study in order to come up with an even more efficient tuning mechanism for the adjustment of the proposed $PI^{\lambda}DND^2N^2$ controller parameters. Therefore, a novel metaheuristic algorithm is also proposed in this paper for the first time by boosting the structure of a recent metaheuristic algorithm named weighted mean of vectors (INFO) algorithm [23] with the aid of elite opposition-based learning scheme [24] and the pattern search method [25]. The proposed boosted INFO (b-INFO) algorithm was constructed such that excellent balance between exploration and exploitation stages was achieved. In this way, a more efficient algorithm was constructed to adjust the parameters of the $PI^{\lambda}DND^2N^2$ controller to optimal values for the vehicle cruise control system.

To verify the effectiveness of the proposed b-INFO algorithm, classical benchmark functions having unimodal, multimodal and fixed-dimensional multimodal properties (twenty-three test functions in total) were employed and the performance evaluation of the b-INFO algorithm was comparatively performed against original form of INFO algorithm [23], marine predators algorithm [26] and gravitational search algorithm [27]. The assessment on the test functions confirmed the excellent ability of the proposed b-INFO algorithm in terms of exploration and exploitation, thus, reaches improved solution quality. On the other hand, the comparative time complexity analysis showed a negligible higher run time for the proposed b-INFO algorithm compared to the original INFO algorithm which is expected due to inclusion of elite opposition-based learning and pattern search mechanisms, however, has less run time compared to marine predators and gravitational search algorithms.

A sensitivity analysis was performed to reach the good performance, and the best suitable values for the parameters of the algorithm were determined. A suitable objective function was then employed, and its value was minimized to reach optimal parameters of the $PI^{\lambda}DND^2N^2$ controller. Several analyses such as statistical, time response and robustness for different operating speeds were performed and the superior performance of the algorithm was demonstrated. To further evaluate the efficiency of the proposed b-INFO algorithm based $PI^{\lambda}DND^2N^2$ controller for the vehicle cruise control system, the most recently reported methods of genetic algorithm based PID [4], ant lion optimizer based PID [5], atom search optimization algorithm based PID [18], arithmetic optimization algorithm based PID [20], slime mould algorithm based PID [20], Lévy flight distribution algorithm based PID [20], manta ray foraging optimization based PID [20] and hunger games search based PID [20] along with Harris hawks optimization based PID and FOPID [22] controllers were employed. The related comparisons further demonstrated the excellent ability of the proposed method for the vehicle cruise control system. Considering the above discussion, the contributions of this work can briefly be listed as follows:

- A state-of-the-art metaheuristic algorithm is proposed by augmenting the performance of the INFO algorithm using PS and EOBL mechanisms.
- The resulting b-INFO algorithm surpasses the original INFO, marine predators, and gravitational search algorithms in terms of performance on benchmark functions, including unimodal, multimodal, and fixed-dimensional multimodal functions.
- A novel $PI^{\lambda}DND^2N^2$ controller is proposed as a more efficient control structure for vehicle cruise control system.
- This work presents the first report of a $PI^{\lambda}DND^2N^2$ controller's implementation for vehicle cruise control system, underscoring the novelty and significance of this research.
- The proposed method's performance is compared against a range of recent approaches. Results demonstrate that the b-INFO algorithm-based $PI^{\lambda}DND^2N^2$ controller is the most efficient and superior method for controlling a vehicle cruise control system.
- The proposed method's exceptional ability is further confirmed by comparisons with the genetic algorithm, ant lion optimizer, atom search optimizer, arithmetic optimization algorithm, slime mold algorithm, Lévy flight distribution algorithm, manta ray foraging optimization, and hunger games search-based PID, along with Harris hawks optimization-based PID and FOPID controllers.
- Considering the above list, this work marks a remarkable milestone toward safer and more efficient vehicle cruise control systems.

2 INFO Algorithm

The INFO algorithm in question is a cutting-edge, population-based metaheuristic approach that operates by considering vectors as potential solutions [23]. Through sophisticated calculations involving the weighted mean of a set of vectors within the search space, the INFO algorithm generates a dynamic sequence of steps that involve updating the positions of these vectors. The process is refined through a series of intricate stages that include vector combining, local search, and updating rule, which all contribute to the overall efficacy of the algorithm. The initialization phase of the INFO algorithm is a crucial stage that relies on the power of Eq. (1), a sophisticated equation that randomly generates a population of vectors. At this stage, the algorithm harnesses the full potential of its arsenal, with Np representing the population of vector, D symbolizing the dimension of the search space, and l taking on the values of $1, 2, \ldots, Np$. With these complex mechanisms working in tandem, the INFO algorithm stands as a true testament to the cutting edge of computational science.

$$X_{l,j}^{g} = \left\{ x_{l,1}^{g}, x_{l,2}^{g}, \ldots, x_{l,D}^{g} \right\} \tag{1}$$

The weighted mean factor (δ) and the scaling factor (σ) are also employed in the initialization stage. The latter two variables are respectively defined in Eqs. (2) and (3) where $\beta = 2e^{-4(g/Maxg)}$ and $\alpha = ce^{-d(g/Maxg)}$.

$$\delta = 2\beta \times rand - \beta \tag{2}$$

$$\sigma = 2\alpha \times rand - \alpha \tag{3}$$

In the latter definitions, g denotes the current generation, $Maxg$ represents the maximum number of generations (iterations) and c is a constant number of 2 whereas d is a constant number of 4. The variables of δ and σ are not adjusted by the user and they change dynamically through generations. The scaling factor serves to amplify the resulting vector by utilizing the updating procedure, which relies on the size of the search domain. It is employed to scale the weighted average of vectors. Its value is determined based on the feasible search space of the problems at hand and is subsequently reduced following an exponential formula. The population diversity is increased with the $MeanRule$, defined in the following equation.

$$MeanRule = r \times WM1_{l}^{g} + (1 - r) \times WM2_{l}^{g} \tag{4}$$

The terms of $WM1_{l}^{g}$ and $WM2_{l}^{g}$ have the following definitions involving several terms, including a random number r within $[0, 0.5]$, a small constant number ε, a normally distributed random value rand, and randomly selected integer numbers $\alpha 1$, $\alpha 2$, $\alpha 3$ (where $\alpha 1 \neq \alpha 2 \neq \alpha 3$) from $[1, Np]$.

$$WM1_{l}^{g} = \delta \times \frac{w_1\left(x_{\alpha 1} - x_{\alpha 2}\right) + w_2\left(x_{\alpha 1} - x_{\alpha 3}\right) + w_3\left(x_{\alpha 2} - x_{\alpha 3}\right)}{w_1 + w_2 + w_3 + \varepsilon} + \varepsilon \times rand \tag{5}$$

$$WM2_{l}^{g} = \delta \times \frac{w_1\left(x_{bs} - x_{bt}\right) + w_2\left(x_{bs} - x_{ws}\right) + w_3\left(x_{bt} - x_{ws}\right)}{w_1 + w_2 + w_3 + \varepsilon} + \varepsilon \times rand \tag{6}$$

Additionally, the wavelet functions w_1, w_2 and w_3 [23] are used to manipulate these terms, where x_{bs}, x_{bt} and x_{ws} represent the best, better, and worst solutions amongst the vectors, respectively. Furthermore, the updating rule also integrates a convergence acceleration (CA) component, as defined below:

$$CA = randn \times \frac{\left(x_{bs} - x_{\alpha 1}\right)}{\left(f\left(x_{bs}\right) - f\left(x_{\alpha 1}\right) + \varepsilon\right)} \tag{7}$$

where *randn* is a random number with normal distribution. The latter definition can be used to calculate new vector using the following expression.

$$z_l^g = x_l^g + \sigma \times MeanRule + CA \tag{8}$$

The updating rule based on x_{bs}, x_{bt}, x_l^g and $x_{\alpha 1}^g$ is defined as follows in order to obtain new vectors of $z1_l^g$ and $z2_l^g$ in the g^{th} generation. For a random number less than 0.5, the Eqs. (9) and (10) are used; otherwise, Eqs. (11) and (12) are used for calculation.

$$z1_l^g = x_l^g + \sigma \times MeanRule + randn \times \frac{\left(x_{bs} - x_{\alpha 1}^g\right)}{\left(f\left(x_{bs}\right) - f\left(x_{\alpha 1}^g\right) + 1\right)} \tag{9}$$

$$z2_l^g = x_{bs} + \sigma \times MeanRule + randn \times \frac{\left(x_{\alpha 1}^g - x_b^g\right)}{\left(f\left(x_{\alpha 1}^g\right) - f\left(x_{\alpha 2}^g\right) + 1\right)} \tag{10}$$

$$z1_l^g = x_\alpha^g + \sigma \times MeanRule + randn \times \frac{\left(x_{\alpha 2}^g - x_{\alpha 3}^g\right)}{\left(f\left(x_{\alpha 2}^g\right) - f\left(x_{\alpha 3}^g\right) + 1\right)} \tag{11}$$

$$z2_l^g = x_{bt} + \sigma \times MeanRule + randn \times \frac{\left(x_{\alpha 1}^g - x_{\alpha 2}^g\right)}{\left(f\left(x_{\alpha 1}^g\right) - f\left(x_{\alpha 2}^g\right) + 1\right)} \tag{12}$$

The vector combining stage of the algorithm amalgamates the obtained vectors of $z1_l^g$ and $z2_l^g$ with the vector of x_l^g to produce the new vector u_l^g, which adheres to certain pre-defined conditions. The parameter μ, which signifies a normally distributed random value multiplied by 0.05, is also taken into account in this process.

if rand < 0.5

if rand < 0.5

$$u_l^g = z1_l^g + \mu \cdot \left| z1_l^g - z2_l^g \right| \tag{13}$$

else

$$u_l^g = z2_l^g + \mu \cdot \left| z1_l^g - z2_l^g \right| \tag{14}$$

end

else

$$u_l^g = x_l^g \tag{15}$$

end

The exploitation process is performed through the vector combining stage; nevertheless, the INFO algorithm goes the extra mile to boost its effectiveness by implementing a local search stage to evade the pitfalls of being trapped in local optima. In this later stage, the algorithm harnesses the power of the global best position (x_{best}^g) and the mean-based rule described in Eq. (16) to perform the local search operator.

$$WM = \frac{x_1 \times w_1 + x_2 \times w_2}{w_1 + w_2} \tag{16}$$

A new vector around x_{best}^g can be produced as follows:

if rand < 0.5

if rand < 0.5

$$u_l^g = x_{bs} + randn \times \left(MeanRule + randn \times \left(x_{bs}^g - x_{\alpha 1}^g\right)\right) \tag{17}$$

else

$$u_l^g = x_{rnd} + randn \times \left(MeanRule + randn \times \left(v_1 \times x_{bs} - v_2 \times x_{rnd}\right)\right) \tag{18}$$

end

end

The INFO algorithm aims to increase the diversity of the search space by introducing a new solution, denoted as x_{rnd}, which is randomly generated using a combination of the best and better solutions. Specifically, x_{rnd} is defined as $x_{rnd} = \varphi \times x_{avg} + (1 - \varphi) \times \left(\varphi \times x_{bt} + (1 - \varphi) \times x_{bs}\right)$. Here, the term φ is a randomly generated number within the range of (0, 1) and $x_{avg} = \left(x_a + x_b + x_3\right)/3$, while v_1 and v_2 are two additional random numbers that are used to further emphasize the impact of the best position on the vector. The values of v_1 and v_2 are determined using a randomly generated number p within the range of (0, 1).

$$v_1 = \begin{cases} 2 \times rand, & p > 0.5 \\ 1, & otherwise \end{cases} \tag{19}$$

$$v_2 = \begin{cases} rand, & p < 0.5 \\ 1, & otherwise \end{cases} \tag{20}$$

The flowchart of the INFO algorithm is provided in Fig. 1.

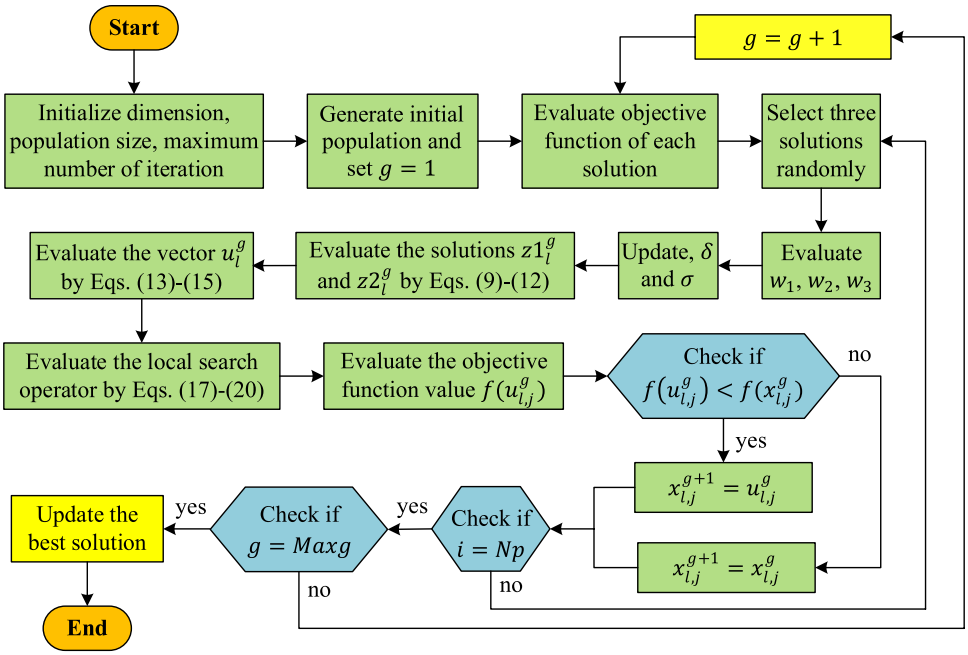


Fig. 1 Flowchart of INFO algorithm

3 A Novel Approach for Improving Performance of INFO Algorithm

3.1 Elite Opposition-Based Learning Mechanism

The opposition-based learning (OBL) scheme, proposed by Tizhoosh in 2005 [28], has been an efficacious machine learning technique to enhance the performance of metaheuristic algorithms, as suggested by recent studies [29]. A more advanced version of the OBL mechanism, known as the elite OBL (EOBL) strategy, has also been introduceed [24]. The OBL approach leverages the opposite solutions of the current individuals in conjunction with their current states, resulting in more effective exploration [30]. In contrast, the EOBL strategy combines the best individuals with the current ones, generates the opposite solutions of the elite individuals [31], and evaluates their fitness values. From a mathematical standpoint, if we consider $X = \langle x_1, x_2 \dots, x_v \rangle$ as an elite candidate solution with v decision variables, then the elite opposition-based solution (X^o) is defined as follows:

$$X^o = \langle x_1^o, x_2^o \dots, x_v^o \rangle \tag{21}$$

where $x_i^o = \delta(da_i + db_i) - x_i$ and δ is a parameter within (0, 1) which is used to control the opposition magnitude. The dynamic boundaries are denoted by da_i and db_i which are defined as

$$da_i = min(x_i), db_i = max(x_i) \tag{22}$$

The EOBL strategy employs the following rule to prevent exceeding the boundaries $[Lb_i, Ub_i]$ for any opposite decision variable where $rand(Lb_i, Ub_i)$ denotes a random number within (Lb_i, Ub_i).

$$x_i^o = rand(Lb_i, Ub_i), \quad \text{if} \quad x_i^o < Lb_i \quad \text{or} \quad x_i^o > Ub_i \tag{23}$$

3.2 Pattern Search Method

The pattern search (PS) is a derivative-free method having good exploitation capability [25]. In the PS method, an initial point (S_0) is defined by the user which becomes the starting point for the search [32]. The size of the mesh, for the first iteration, is considered as 1 and the pattern (direction) vectors are constructed as: $S_0 + [0\,1]$, $S_0 + [1\,0]$, $S_0 + [-1\,0]$ and $S_0 + [0\ -\ 1]$. This procedure helps generating new mesh points. The objective functions are then calculated for those generated points which continues until a smaller value than S_0 is found. Finding a smaller value such as $f(S_1) < f(S_0)$ means the poll is successful. In such a case, the related point is set as a source point. After the successful poll, the PS algorithm performs the expansion operation in the second iteration by multiplying the current mesh size with 2 such that the new points are produced as $S_1 + 2 \times [0\,1]$, $S_1 + 2 \times [1\,0]$, $S_1 + 2 \times [-1\,0]$ and $S_1 + 2 \times [0\ -\ 1]$. The expanding stage keeps operating provided a newer point with lower objective function is achieved. Otherwise, the contraction stage is performed which reduces the mesh size by multiplying it with 0.5.

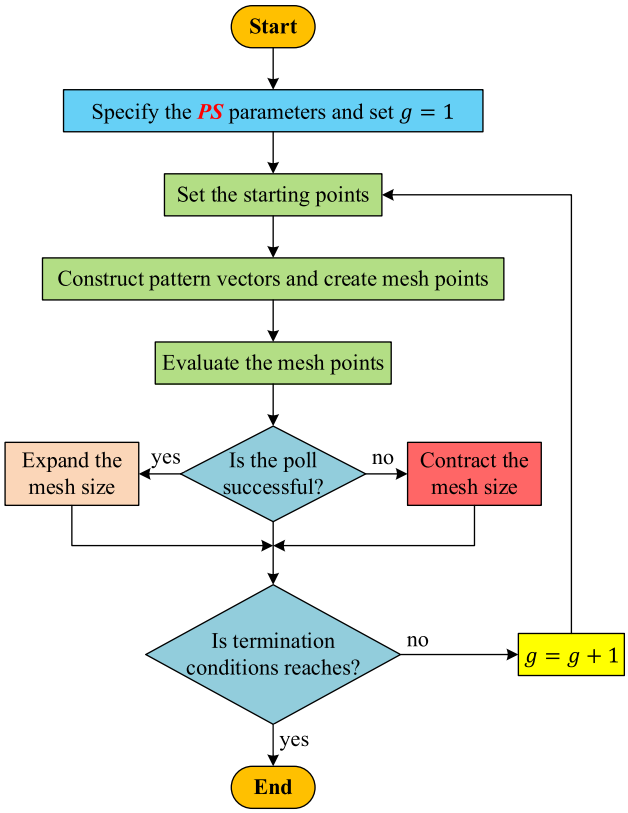


Fig. 2 Flowchart of PS method

The overall process continues until the termination condition is met. In this study, the following parameter values were used: initial mesh size = 1, mesh expansion factor = 2, mesh contraction factor = 0.5, all tolerances = 10^{-6}. The flowchart of the PS algorithm is provided in Fig. 2.

3.3 Proposed Boosted INFO Algorithm

In this study, with the aim of reaching a better exploration and exploitation capability, the structure of the original form of the INFO algorithm was improved by the integration of the EOBL strategy and the PS method. The proposed b-INFO algorithm uses the PS method to aid enhanced exploitation and employs the EOBL strategy to reach further exploration power. A detailed flowchart of the proposed b-INFO algorithm is provided in Fig. 3. As shown in this flowchart, the proposed b-INFO algorithm starts with the operation of the original INFO algorithm to generate a best solution which is then further improved with the integration of the EOBL strategy. After obtaining N_P best solutions, the PS method operates with the aim of reaching better exploitation power. At this stage, instead of performing the PS method in each iteration, it is operated only twice through complete operation of the algorithm and for each operation it runs for $100 \times D$ iterations where D denotes the dimension size of the problem. Such an overall procedure was constructed after extensive simulations and consequently boosted the ability of the original INFO algorithm significantly.

4 Initial Performance Evaluation

4.1 Employed Benchmark Functions

In this study, the performance of the constructed b-INFO algorithm was tested initially against benchmark functions. In this regard, the unimodal, multimodal, and fixed dimensional multimodal benchmark functions were employed in order to demonstrate the more excellent capacity of the proposed b-INFO algorithm in terms of exploration, exploitation and solution quality as those benchmark functions provide a good platform to test the performance of the algorithms. The name, equation, range, dimensions (D) and optimum point (f_{min}) details of the unimodal, multimodal and fixed-dimensional multimodal benchmark functions are respectively provided in Tables 1, 2 and 3.

4.2 Compared Metaheuristic Algorithms

In this study, marine predators algorithm (MPA) [26] and gravitational search algorithm (GSA) [27] were employed in addition to the original INFO algorithm in order to provide a comparative assessment. Table 4 lists those algorithms and their respective parameters. In addition, each algorithm was run for 30 times.

4.3 Assessment of the Exploitative Behavior

To assess the exploitation power of the proposed b-INFO algorithm, a suite of unimodal benchmark functions listed in Table 1 were employed. The attained results are comprehensively presented in Table 5, where the superior performance of the b-INFO algorithm is evidently manifested by the remarkably low values obtained.

4.4 Assessment of the Explorative Behavior

In the present study, the exploration power and solution quality of the proposed b-INFO algorithm were assessed using both multimodal and fixed-dimensional multimodal benchmark functions provided in Tables 2 and 3. The results of the experiments are presented in a comparative manner in Tables 6 and 7. The numerical results indicate a remarkable performance of the proposed b-INFO algorithm, highlighting its superiority in terms of exploration and solution

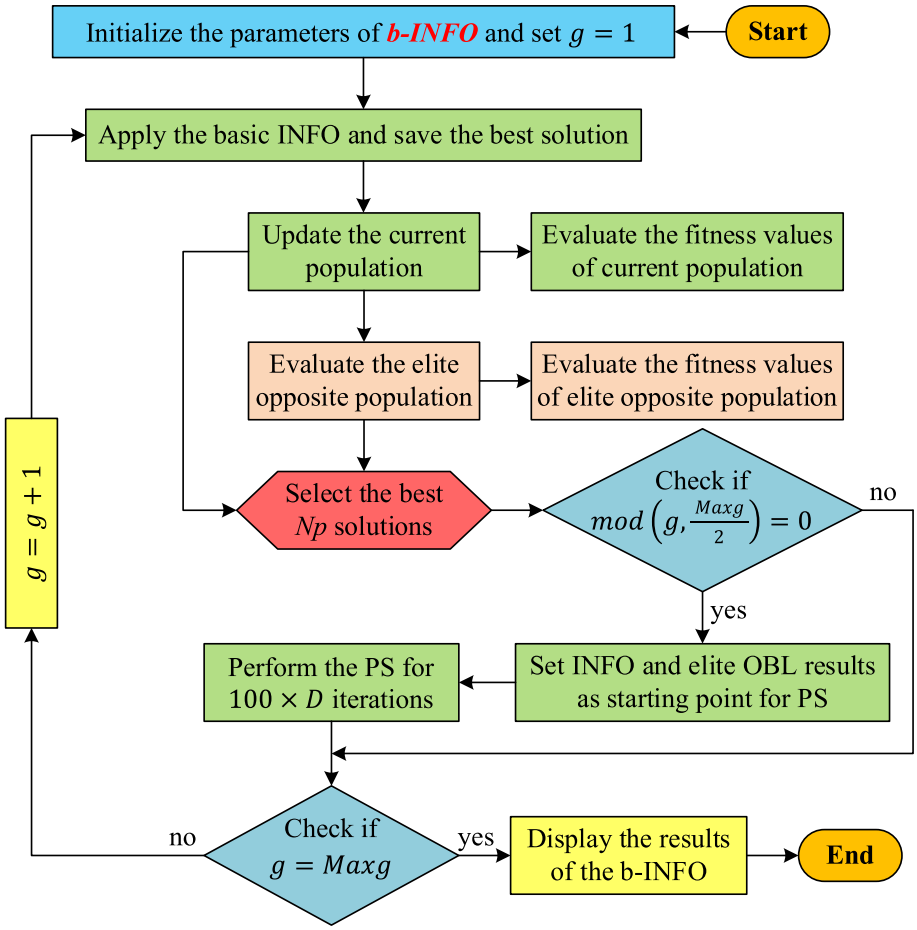


Fig. 3 Flowchart of b-INFO

Table 1 Unimodal benchmark functions

Name	Equation of test function	D	Range	f_{min}
Sphere	$f_1(x) = \sum_{i=1}^{D} x_i^2$	30	$[-100, 100]$	0
Schwefel 2.2	$f_2(x) = \sum_{i=1}^{D} \lvert x_i \rvert + \prod_{i=1}^{D} \lvert x_i \rvert$	30	$[-10, 10]$	0
Schwefel 1.2	$f_3(x) = \sum_{i=1}^{D} \left(\sum_{j=1}^{i} x_j \right)^2$	30	$[-100, 100]$	0
Schwefel 2.21	$f_4(x) = \max_i \{ \lvert x_i \rvert, 1 \le i \le D \}$	30	$[-100, 100]$	0
Rosenbrock	$f_5(x) = \sum_{i=1}^{D-1} \left(100(x_{i+1} - x_i^2)^2 + (x_i - 1)^2 \right)$	30	$[-30, 30]$	0
Step	$f_6(x) = \sum_{i=1}^{D} (x_i + 0.5)^2$	30	$[-100, 100]$	0
Quartic	$f_7(x) = \sum_{i=1}^{D} i x_i^4 + random[0, 1)$	30	$[-1.28, 1.28]$	0

Table 2 Multimodal benchmark functions

Name	Equation of test function	D	Range	f_{min}
Schwefel	$f_8(x) = \sum_{i=1}^{D} \left(-x_i \sin\left(\sqrt{\lvert x_i \rvert}\right)\right)$	30	$[-500, 500]$	$-1.2569E+04$
Rastrigin	$f_9(x) = \sum_{i=1}^{D} \left[x_i^2 - 10\cos\left(2\pi x_i\right) + 10\right]$	30	$[-5.12, 5.12]$	0
Ackley	$f_{10}(x) = -20exp\left(-0.2\sqrt{\frac{1}{D}\sum_{i=1}^{D} x_i^2}\right) - exp\left(\frac{1}{D}\sum_{i=1}^{D}\cos\left(2\pi x_i\right)\right) + 20 + e$	30	$[-32, 32]$	0
Griewank	$f_{11}(x) = \sum_{i=1}^{D} \frac{x_i^2}{4000} - \prod_{i=1}^{D} \cos\left(\frac{x_i}{\sqrt{i}}\right) + 1$	30	$[-600, 600]$	0
Penalized	$f_{12}(x) = \frac{\pi}{D}\left\{10\sin^2(\pi y_1) + \sum_{i=1}^{D-1}(y_i - 1)^2\left[1 + 10\sin^2(\pi y_{i+1})\right] + (y_D - 1)^2\right\} + \sum_{i=1}^{D} u(x_i, 10, 100, 4)$	30	$[-50, 50]$	0
Penalized2	$f_{13}(x) = 0.1\left\{\sin^2(3\pi x_1) + \sum_{i=1}^{D-1}(x_i - 1)^2\left[1 + \sin^2(3\pi x_{i+1})\right] + (x_D - 1)^2[1 + \sin^2(2\pi x_D)]\right\} + \sum_{i=1}^{D} u(x_i, 5, 100, 4)$	30	$[-50, 50]$	0

Table 3 Fixed-dimensional multimodal benchmark functions

Name	Equation of test function	D	Range	f_{min}
Foxholes	$f_{14}(x) = \left(\frac{1}{500} + \sum_{j=1}^{25} \frac{1}{j + \sum_{i=1}^{2}\left(x_i - a_{ij}\right)^6}\right)^{-1}$	2	$[-65.536, 65.536]$	0.998
Kowalik	$f_{15}(x) = \sum_{i=1}^{11}\left[a_i - \frac{x_1\left(b_i^2 + b_i x_2\right)}{b_i^2 + b_i x_3 + x_4}\right]^2$	4	$[-5, 5]$	3.0749E−04
Six-Hump Camel	$f_{16}(x) = 4x_1^2 - 2.1x_1^4 + \frac{1}{3}x_1^6 + x_1 x_2 - 4x_2^2 + 4x_2^4$	2	$[-5, 5]$	-1.0316
Branin	$f_{17}(x) = \left(x_2 - \frac{5.1}{4\pi^2}x_1^2 + \frac{5}{\pi}x_1 - 6\right)^2 + 10\left(1 - \frac{1}{8\pi}\right)\cos x_1 + 10$	2	$[-5, 10] \times [0, 15]$	0.39789
Goldstein-Price	$f_{18}(x) = \left[1 + \left(x_1 + x_2 + 1\right)^2\left(19 - 14x_1 + 3x_1^2 - 14x_2 + 6x_1 x_2 + 3x_2^2\right)\right]$ $\times\left[30 + \left(2x_1 - 3x_2\right)^2 \times \left(18 - 32x_1 + 12x_1^2 + 48x_2 - 36x_1 x_2 + 27x_2^2\right)\right]$	2	$[-2, 2]$	3
Hartman 3	$f_{19}(x) = -\sum_{i=1}^{4} c_i\, exp\left(-\sum_{j=1}^{3} a_{ij}\left(x_j - p_{ij}\right)^2\right)$	3	$[0, 1]$	-3.8628
Hartman 6	$f_{20}(x) = -\sum_{i=1}^{4} c_i exp\left(-\sum_{j=1}^{6} a_{ij}\left(x_j - p_{ij}\right)^2\right)$	6	$[0, 1]$	-3.322
Shekel 5	$f_{21}(x) = -\sum_{i=1}^{5}\left[\left(X - a_i\right)\left(X - a_i\right)^T + c_i\right]^{-1}$	4	$[0, 10]$	-10.1532
Shekel 7	$f_{22}(x) = -\sum_{i=1}^{7}\left[\left(X - a_i\right)\left(X - a_i\right)^T + c_i\right]^{-1}$	4	$[0, 10]$	-10.4029
Shekel 10	$f_{23}(x) = -\sum_{i=1}^{10}\left[\left(X - a_i\right)\left(X - a_i\right)^T + c_i\right]^{-1}$	4	$[0, 10]$	-10.5364

Table 4 Parameter settings of algorithms for benchmark functions

Algorithm	Population size	Maximum iteration number	Values of other parameters
b-INFO	30	500	$c = 2, d = 4$
INFO	30	500	$c = 2, d = 4$
MPA	30	500	$FADs = 0.2, P = 0.5$
GSA	30	500	$G_0 = 100, \alpha = 20$

quality. Overall, the findings provide strong evidence for the excellent capability of the b-INFO algorithm.

4.5 Wall-Clock Time Analysis

The proposed b-INFO algorithm was also investigated comparatively in terms of the run-time. In this regard, all the 23 benchmark functions were employed, and a comparative analysis was performed by running all algorithms. The respective results are numerically presented in Table 8. As can be observed, for each benchmark function the INFO algorithm takes the shortest time per run. The proposed

Table 5 Statistical results of the unimodal benchmark functions from b-INFO and the other three algorithms

Function	Algorithm	Mean	SD	Best	Worst
$f_1(x)$	b-INFO	0	0	0	0
	INFO	1.1744E−53	9.6057E−54	1.9696E−54	3.7923E−53
	MPA	5.5835E−23	7.3675E−23	6.7593E−26	3.3077E−22
	GSA	2.2404E−16	8.8525E−17	9.2743E−17	4.5343E−16
$f_2(x)$	b-INFO	1.1547E−236	0	5.1601E−251	2.4262E−235
	INFO	1.1781E−26	3.4620E−27	3.0611E−27	1.9534E−26
	MPA	2.8814E−13	2.2700E−13	2.2952E−14	9.0809E−13
	GSA	2.0554E−01	5.8235E−01	5.9408E−08	2.4005E+00
$f_3(x)$	b-INFO	0	0	0	0
	INFO	1.4053E−50	8.6069E−51	1.0925E−51	3.1106E−50
	MPA	1.6806E−04	2.9945E−04	3.0260E−07	1.4848E−03
	GSA	9.8702E+02	3.2744E+02	4.6177E+02	1.7710E+03
$f_4(x)$	b-INFO	1.2513E−241	0	5.9480E−256	3.6133E−240
	INFO	1.7831E−27	1.0192E−27	2.3347E−28	4.8431E−27
	MPA	3.6156E−09	1.9985E−09	8.4518E−10	8.2999E−09
	GSA	7.1809E+00	1.7089E+00	4.7645E+00	1.1152E+01
$f_5(x)$	b-INFO	1.6309E−07	4.6160E−07	7.6611E−11	2.3225E−06
	INFO	2.2574E+01	7.0170E−01	2.1101E+01	2.3725E+01
	MPA	2.5297E+01	3.4097E−01	2.4916E+01	2.6112E+01
	GSA	7.7634E+01	1.3195E+02	2.4154E+01	7.3518E+02
$f_6(x)$	b-INFO	1.0658E−14	2.9714E−14	1.3857E−17	1.5776E−13
	INFO	4.9097E−09	9.0037E−09	7.4755E−11	3.8939E−08
	MPA	2.5825E−06	1.0116E−05	2.0834E−08	4.9384E−05
	GSA	7.7067E−02	3.2827E−01	1.0372E−16	1.7633E+00
$f_7(x)$	b-INFO	5.2688E−05	4.1809E−05	5.8502E−06	1.5826E−04
	INFO	1.7498E−03	1.4290E−03	2.9336E−04	6.0973E−03
	MPA	1.5595E−03	7.4569E−04	3.0192E−04	3.5190E−03
	GSA	7.7963E−02	4.1596E−02	2.4128E−02	2.1844E−01

b-INFO algorithm has a slightly higher run time, due to inclusion of EOBL and PS mechanisms (between 3 and 5% depending on the benchmark function), compared to INFO algorithm. however, it reaches a significantly improved solution quality. In addition, the proposed b-INFO algorithm has less run time compared to MPA and GSA algorithms.

4.6 Sensitivity Analysis

A sensitivity analysis was also carried out in this study in order to determine the best suitable values for the adjustment of c and d parameters of the proposed b-INFO algorithm. In this regard, c and d parameters were assigned five different values $(2, 4, 6, 8, 10)$ separately which created a combination of $5 \times 5 = 25$ different designs. The analysis was performed against $f_5(x)$ (unimodal), $f_{12}(x)$ (multimodal) and $f_{20}(x)$ (fixed-dimensional multimodal) benchmark functions. The respective parameter combinations and the obtained statistical metrics are shown in Table 9. Considering the presented numerical results, it can easily be spotted that there are different specific combinations (shown in bold for case no 2, 5, 6, 11, 16, 18 and 22) to reach good values for $f_{20}(x)$, however, the best combination for the parameter settings is achieved with $c = 2$ and $d = 4$ (case no 2) which provided the best results for all types of the benchmark functions. Therefore, in this study, the c and d parameters were adjusted to be 2 and 4, respectively.

Table 6 Statistical results of the multimodal benchmark functions from b-INFO and the other three algorithms

Function	Algorithm	Mean	SD	Best	Worst
$f_8(x)$	b-INFO	−1.2547E+04	1.2251E+02	−1.2569E+04	−1.1898E+04
	INFO	−8.5957E+03	7.7703E+02	−1.0120E+04	−6.8218E+03
	MPA	−8.9596E+03	4.8037E+02	−9.9781E+03	−7.9118E+03
	GSA	−2.5124E+03	3.8477E+02	−3.3933E+03	−1.8654E+03
$f_9(x)$	b-INFO	0	0	0	0
	INFO	0	0	0	0
	MPA	0	0	0	0
	GSA	3.0180E+01	8.8157E+00	1.4924E+01	5.1738E+01
$f_{10}(x)$	b-INFO	8.8818E−16	0	8.8818E−16	8.8818E−16
	INFO	8.8818E−16	0	8.8818E−16	8.8818E−16
	MPA	1.5093E−12	8.5077E−13	2.5668E−13	3.8058E−12
	GSA	8.3199E−02	3.1749E−01	7.7121E−09	1.3404E+00
$f_{11}(x)$	b-INFO	0	0	0	0
	INFO	0	0	0	0
	MPA	0	0	0	0
	GSA	2.8574E+01	8.8725E+00	1.6300E+01	5.7105E+01
$f_{12}(x)$	b-INFO	1.8601E−16	7.2546E−16	1.1892E−18	3.9569E−15
	INFO	6.9107E−03	3.7851E−02	6.9320E−12	2.0732E−01
	MPA	2.1410E−06	7.2848E−06	2.3180E−09	3.4628E−05
	GSA	2.1652E+00	1.2525E+00	3.9010E−01	6.2088E+00
$f_{13}(x)$	b-INFO	5.4748E−15	1.1709E−14	1.1888E−17	4.6266E−14
	INFO	6.3957E−02	5.9256E−02	6.2210E−09	2.0724E−01
	MPA	1.7282E−02	3.4376E−02	2.1114E−08	1.6077E−01
	GSA	9.8490E+00	7.3372E+00	4.6973E−01	3.5408E+01

5 Vehicle Cruise Control System's Mathematical Model

The precise control of a vehicle's velocity is achieved through the utilization of its cruise control system, which continuously adjusts the engine throttle angle (u) to regulate the vehicle's speed (v) to a pre-set reference speed (v_{ref}). The underlying dynamics of a vehicle's longitudinal motion can be mathematically formulated as per the established work of Lewis and Houghton [33]:

$$F_d = M\frac{dv}{dt} + F_a + F_g \tag{24}$$

where F_d, F_a, F_g and $M(dv/dt)$ stand for the engine's drive force, aerodynamic drag, the climbing resistance and the inertia force, respectively. The dynamic model of the vehicle cruise control system is shown in Fig. 4 where the terms of θ, v_w, C_a and M stands for road angle, wind gust speed, the aerodynamic drag coefficient and the total mass of the vehicle and the passengers.

For the initial assessment, the vehicle is assumed to operate at a speed of 30 km/h without any wind gust speed and climbing resistance. The system's state model can then be described as [33]:

$$\dot{v} = \frac{1}{M}(F_d - C_a v^2) \tag{25}$$

$$\dot{F}_d = \frac{1}{T}(C_1 u(t-\tau) - F_d) \tag{26}$$

For an equilibrium state with a nominal operating speed ($v_{ref} = v_0 = 30$ km/h), a nominal drive force (F_{d0}) with a nominal throttle position (u_0), which are defined as follows, are required.

$$F_{d0} = C_a {v_0}^2 \tag{27}$$

$$u_0 = F_{d0}/C_1 \tag{28}$$

Linearizing the model around the stated set points would help obtaining the following definitions [33]:

$$\delta\dot{v} = -\frac{2C_a v_0}{M}\delta v + \frac{1}{M}\delta F_d \tag{29}$$

Table 7 Statistical results of the fixed-dimensional multimodal benchmark functions from b-INFO and the other three algorithms

Function	Algorithm	Mean	SD	Best	Worst
$f_{14}(x)$	b-INFO	9.9800E−01	0	9.9800E−01	9.9800E−01
	INFO	1.4930E+00	1.1237E+00	9.9800E−01	5.9288E+00
	MPA	9.9800E−01	0	9.9800E−01	9.9800E−01
	GSA	6.9381E+00	4.3521E+00	9.9800E−01	1.6441E+01
$f_{15}(x)$	b-INFO	3.0749E−04	0	3.0749E−04	3.0749E−04
	INFO	3.1037E−03	6.8925E−03	3.0749E−04	2.0363E−02
	MPA	3.0749E−04	0	3.0749E−04	3.0749E−04
	GSA	4.1392E−03	2.6573E−03	1.9828E−03	1.5888E−02
$f_{16}(x)$	b-INFO	−1.0316E+00	0	−1.0316E+00	−1.0316E+00
	INFO	−1.0316E+00	0	−1.0316E+00	−1.0316E+00
	MPA	−1.0316E+00	0	−1.0316E+00	−1.0316E+00
	GSA	−1.0316E+00	0	−1.0316E+00	−1.0316E+00
$f_{17}(x)$	b-INFO	3.9789E−01	0	3.9789E−01	3.9789E−01
	INFO	3.9789E−01	0	3.9789E−01	3.9789E−01
	MPA	3.9789E−01	0	3.9789E−01	3.9789E−01
	GSA	3.9789E−01	0	3.9789E−01	3.9789E−01
$f_{18}(x)$	b-INFO	3.0000E+00	0	3.0000E+00	3.0000E+00
	INFO	3.0000E+00	0	3.0000E+00	3.0000E+00
	MPA	3.0000E+00	0	3.0000E+00	3.0000E+00
	GSA	3.0000E+00	0	3.0000E+00	3.0000E+00
$f_{19}(x)$	b-INFO	−3.8628E+00	0	−3.8628E+00	−3.8628E+00
	INFO	−3.8628E+00	0	−3.8628E+00	−3.8628E+00
	MPA	−3.8628E+00	0	−3.8628E+00	−3.8628E+00
	GSA	−3.8628E+00	0	−3.8628E+00	−3.8628E+00
$f_{20}(x)$	b-INFO	−3.3220E+00	0	−3.3220E+00	−3.3220E+00
	INFO	−3.2705E+00	5.9926E−02	−3.3220E+00	−3.2031E+00
	MPA	−3.3220E+00	0	−3.3220E+00	−3.3220E+00
	GSA	−3.3140E+00	3.0497E−02	−3.3220E+00	−3.2009E+00
$f_{21}(x)$	b-INFO	−1.0153E+01	0	−1.0153E+01	−1.0153E+01
	INFO	−9.7323E+00	1.6323E+00	−1.0153E+01	−2.6305E+00
	MPA	−1.0153E+01	0	−1.0153E+01	−1.0153E+01
	GSA	−6.0672E+00	3.7223E+00	−1.0153E+01	−2.6305E+00
$f_{22}(x)$	b-INFO	−1.0403E+01	0	−1.0403E+01	−1.0403E+01
	INFO	−8.9530E+00	2.9758E+00	−1.0403E+01	−2.7659E+00
	MPA	−1.0403E+01	0	−1.0403E+01	−1.0403E+01
	GSA	−9.9120E+00	1.3899E+00	−1.0403E+01	−4.5015E+00
$f_{23}(x)$	b-INFO	−1.0536E+01	0	−1.0536E+01	−1.0536E+01
	INFO	−8.5051E+00	3.4378E+00	−1.0536E+01	−2.4217E+00
	MPA	−1.0536E+01	0	−1.0536E+01	−1.0536E+01
	GSA	−1.0266E+01	1.4815E+00	−1.0536E+01	−2.4217E+00

$$\delta \dot{F}_d = -\frac{1}{T}\delta F_d + \frac{C_1}{T}\delta u(t-\tau) \tag{30}$$

The following transfer function can be obtained for the linearized model of the vehicle cruise control system where $C = \frac{C_1}{MT\tau}$, $p_1 = -2\frac{C_a v_0}{M}$, $p_2 = -\frac{1}{T}$ and $p_3 = -\frac{1}{\tau}$.

$$G(s) = \frac{\Delta V(s)}{\Delta U(s)} = \frac{C}{(s-p_1)(s-p_2)(s-p_3)} \tag{31}$$

In this paper, the parameter values presented in Table 10 were employed in order to present a fair comparison with the works presented in the literature.

Table 8 Comparison of the run-time of b-INFO and other algorithms

Function	b-INFO	INFO	MPA	GSA
$f_1(x)$	0.7812	0.7515	1.3046	1.3775
$f_2(x)$	0.8928	0.8516	1.5080	1.3464
$f_3(x)$	1.4350	1.3753	2.6456	1.9170
$f_4(x)$	0.7854	0.7604	1.3419	1.3377
$f_5(x)$	0.9209	0.8841	1.4277	1.3825
$f_6(x)$	0.8054	0.7724	1.2897	1.2297
$f_7(x)$	0.9630	0.9187	1.4490	1.5041
$f_8(x)$	1.0678	1.0308	1.3366	1.2925
$f_9(x)$	1.0837	1.0387	1.3994	1.3130
$f_{10}(x)$	1.1282	1.0770	1.6251	1.2967
$f_{11}(x)$	1.1131	1.0605	1.5210	1.4560
$f_{12}(x)$	1.4315	1.3766	1.9052	1.7490
$f_{13}(x)$	1.3566	1.3105	1.9207	1.7138
$f_{14}(x)$	1.7574	1.6955	2.8809	1.9427
$f_{15}(x)$	1.0766	1.0333	1.4616	1.1885
$f_{16}(x)$	0.9857	0.9469	1.2936	1.1549
$f_{17}(x)$	1.0004	0.9564	1.2428	1.1385
$f_{18}(x)$	1.0319	0.9885	1.2523	1.1939
$f_{19}(x)$	1.1742	1.1292	1.4100	1.2917
$f_{20}(x)$	1.0632	1.0197	1.5335	1.3165
$f_{21}(x)$	1.1995	1.1452	1.4869	1.3664
$f_{22}(x)$	1.1792	1.1384	1.8400	1.3842
$f_{23}(x)$	1.2559	1.2035	1.7149	1.5215

6 A Novel Controller for Vehicle Cruise Control System

6.1 Proposed $PI^{\lambda}DND^2N^2$ Controller

A PID controller has a wider implementation due to several advantages such as being easy to implement, having a simple structure and providing good performance [34]. A PID controller has three parameters (K_P, K_I and K_D) which yields the following transfer function.

$$C_{PID}(s) = K_P + \frac{K_I}{s} + K_D s \tag{32}$$

Despite its wider implementation, a PID controller cannot provide best performance for the dynamic and more complex problems as effectively as its fractional counterpart called FOPID controller [35]. The latter one has additional integration (λ) and derivative (μ) orders which helps increasing the stability and robustness [36]. The transfer function of a FOPID controller can be defined as follows by considering the latter statement.

$$C_{FOPID}(s) = K_P + \frac{K_I}{s^{\lambda}} + K_D s^{\mu} \tag{33}$$

Apart from a FOPID controller, a $PIDD^2$ controller [37] having four parameters (K_P, K_I, K_D and K_{DD}) can also alternatively be used. The transfer function of the latter controller is provided as follows.

$$C_{PIDD^2}(s) = K_P + \frac{K_I}{s} + K_D s + K_{DD} s^2 \tag{34}$$

The additional second-order derivative (K_{DD}) term helps reaching improved phase margin, steady state accuracy, and stability [38]. Considering the abilities of those controllers, this study employs a $PI^{\lambda}DND^2N^2$ controller [11] which has an additional fractional order for the integrator and low pass filters for derivative terms. The transfer function of the employed controller is provided as follows.

$$C_{PI^{\lambda}DND^2N^2}(s) = K_P + \frac{K_I}{s^{\lambda}} + K_D \frac{sN_1}{s+N_1} + K_{DD}\left(\frac{sN_2}{s+N_2}\right)^2 \tag{35}$$

The advantage of the employed $PI^{\lambda}DND^2N^2$ controller is that it can effectively reduce the overshoot, settling and rise time of the system [12]. Besides, the additional two low pass filters allow the derivative terms to appropriately reduce the high frequency gain and noise [11].

The calculations for the fractional integrator were performed with the FOMCON toolbox [39] and the limits for the controller parameters were arranged as $1 \le K_P \le 6$, $0.1 \le K_I \le 0.5$, $1 \le K_D \le 6$, $0.1 \le K_{DD} \le 0.5$, $0.5 \le \lambda \le 1.5$, $10 \le N_1 \le 1000$ and $10 \le N_2 \le 1000$. The block diagram of the $PI^{\lambda}DND^2N^2$ controller is shown in Fig. 5. In the respective figure, the input represents the error between the reference speed and actual speed.

6.2 $PI^{\lambda}DND^2N^2$ Controlled Vehicle Cruise Control System

The block diagram shown in Fig. 6 presents a $PI^{\lambda}DND^2N^2$ controlled vehicle cruise control system. As can be seen, the system consists of a closed loop feedback loop where $\Delta V_{ref}(s)$ represents the commanded speed and $\Delta V(s)$ is the actual operating speed. In this study, the respective block diagram was considered to perform analysis.

7 A Novel Design Approach and Comparative Simulation Results

7.1 Objective Function and Implementation of b-INFO Algorithm

To make use of the advantage of the proposed b-INFO algorithm and the $PI^{\lambda}DND^2N^2$ controller for the vehicle cruise

Table 9 Sensitivity analysis of b-INFO's control parameters with different benchmark functions

Case no	Parameter setting	$f_5(x)$ (Rosenbrock)		$f_{12}(x)$ (Penalized)		$f_{20}(x)$ (Hartman 6)	
		Mean	Std	Mean	Std	Mean	Std
1	$c = 2, d = 2$	2.7005E−07	5.1965E−07	3.9849E−16	8.9597E−16	−3.2744E+00	6.5120E−02
2	$\boldsymbol{c = 2, d = 4}$	**1.6309E−07**	**4.6160E−07**	**1.8601E−16**	**7.2546E−16**	**−3.3220E+00**	**0**
3	$c = 2, d = 6$	1.6659E−07	5.1881E−07	6.4175E−16	9.1030E−16	−3.2982E+00	5.3171E−02
4	$c = 2, d = 8$	1.7192E−07	6.3258E−07	3.9752E−16	7.4734E−16	−3.3101E+00	3.7597E−02
5	$c = 2, d = 10$	1.8471E−07	5.5456E−07	1.8890E−16	7.7405E−16	**−3.3220E+00**	**0**
6	$c = 4, d = 2$	6.4444E−07	1.2242E−06	1.1178E−15	1.5380E−15	**−3.3220E+00**	**0**
7	$c = 4, d = 4$	2.1040E−07	5.5079E−07	7.1151E−16	1.4486E−15	−3.2625E+00	6.3551E−02
8	$c = 4, d = 6$	1.7366E−07	5.2841E−07	2.9533E−16	7.4246E−16	−3.2923E+00	5.5037E−02
9	$c = 4, d = 8$	2.7235E−07	8.2723E−07	7.4646E−16	1.0603E−15	−3.2923E+00	5.9447E−02
10	$c = 4, d = 10$	3.1088E−07	4.7448E−07	3.6275E−15	6.2501E−15	−3.2625E+00	6.8643E−02
11	$c = 6, d = 2$	6.6477E−07	5.3318E−07	9.0713E−16	2.0032E−15	**−3.3220E+00**	**0**
12	$c = 6, d = 4$	1.6435E−07	7.3828E−07	5.8945E−16	8.2696E−16	−3.2427E+00	6.8643E−02
13	$c = 6, d = 6$	1.6933E−07	4.6400E−07	1.6320E−15	3.0189E−15	−3.2880E+00	5.8014E−02
14	$c = 6, d = 8$	3.8056E−07	7.2571E−07	1.8896E−16	7.4121E−16	−3.3050E+00	4.4937E−02
15	$c = 6, d = 10$	1.6697E−07	4.9594E−07	2.1748E−15	2.3935E−15	−3.2625E+00	6.2090E−02
16	$c = 8, d = 2$	7.8147E−07	1.6785E−06	1.0136E−15	1.9036E−15	**−3.3220E+00**	**0**
17	$c = 8, d = 4$	2.1302E−07	5.2134E−07	6.8407E−16	1.1024E−15	−3.2371E+00	5.8014E−02
18	$c = 8, d = 6$	2.3886E−07	6.5879E−07	9.7268E−16	1.7374E−15	**−3.3220E+00**	**0**
19	$c = 8, d = 8$	2.7109E−07	5.0309E−07	3.5676E−16	7.9906E−16	−3.3022E+00	4.6279E−02
20	$c = 8, d = 10$	1.7640E−07	8.9300E−07	2.5065E−16	8.3013E−16	−3.3121E+00	3.4321E−02
21	$c = 10, d = 2$	1.7198E−07	4.9214E−07	3.5466E−16	7.5177E−16	−3.2946E+00	5.2138E−02
22	$c = 10, d = 4$	3.4304E−07	5.8572E−07	4.4229E−16	7.6395E−16	**−3.3220E+00**	**0**
23	$c = 10, d = 6$	6.5417E−07	9.5526E−07	7.6127E−16	1.2724E−15	−3.2774E+00	6.1533E−02
24	$c = 10, d = 8$	4.7042E−07	6.7568E−07	1.0207E−15	2.2597E−15	−3.2854E+00	5.7114E−02
25	$c = 10, d = 10$	6.5792E−07	1.1925E−06	1.1389E−15	1.4953E−15	−3.2710E+00	6.1058E−02

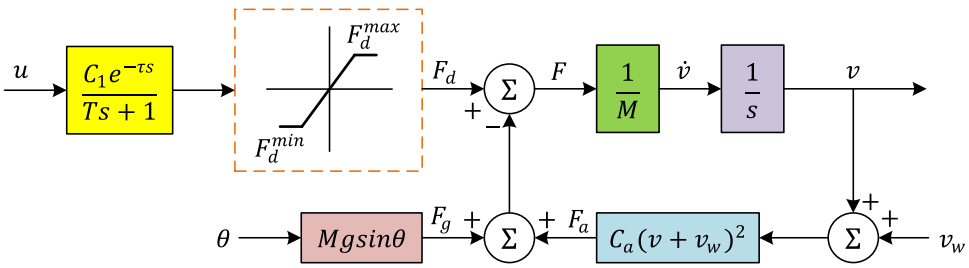


Fig. 4 Dynamic model of the system

Table 10 The employed parameters of the vehicle cruise control system [20]

Parameter	Value	Unit (SI)
C_1 (Actuator constant)	743	–
C_a (Aerodynamic drag coefficient)	1.19	N/(m/s)^2
M (Mass of vehicle and passenger)	1500	kg
τ (Driver reaction time)	0.2	s
T (Observation time)	1	s
g (Gravitational acceleration)	9.8	m/s^2
F_d^{min} (Minimum saturation limit)	−3500	N
F_d^{max} (Maximum saturation limit)	3500	N

control system, the F objective function defined in Eq. (36) was employed.

$$F = (1 - e^{-\sigma})\left(\frac{\%OS}{100} + e_{ss}\right) + e^{-\sigma}(t_s - t_r) \tag{36}$$

where σ denotes a weighting parameter and set to 1 [40], $\%OS$ represents maximum percent overshoot, e_{ss} is the steady state error whereas t_s and t_r are respectively the settling and rise times. Figure 7 depicts the application of the proposed b-INFO algorithm to design a $PI^{\lambda}DND^2N^2$ controller for the vehicle cruise control system. The figure shows

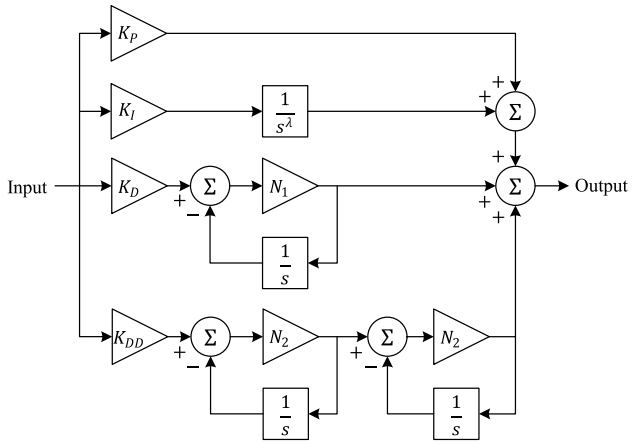


Fig. 5 Block diagram of $PI^{\lambda}DND^2N^2$ controller

that the b-INFO algorithm updates the controller's parameters by considering the F function. The algorithm continues its operation until the maximum number of generations (iterations) is reached, resulting in the optimal parameters of the controller.

7.2 Statistical Analysis and the Obtained Best Parameters of the Controller

Table 11 presents the parameter settings of different algorithms employed in this study in order to perform the comparative analysis for the vehicle cruise control system. In the beginning, the time complexity analysis was performed for the employed algorithms. The respective numerical results for the time complexity are also provided in Table 11. As can be seen, the original INFO algorithm has less time

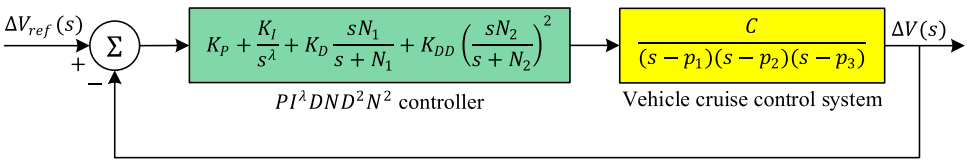


Fig. 6 Block diagram of vehicle cruise control system with $PI^{\lambda}DND^2N^2$ controller

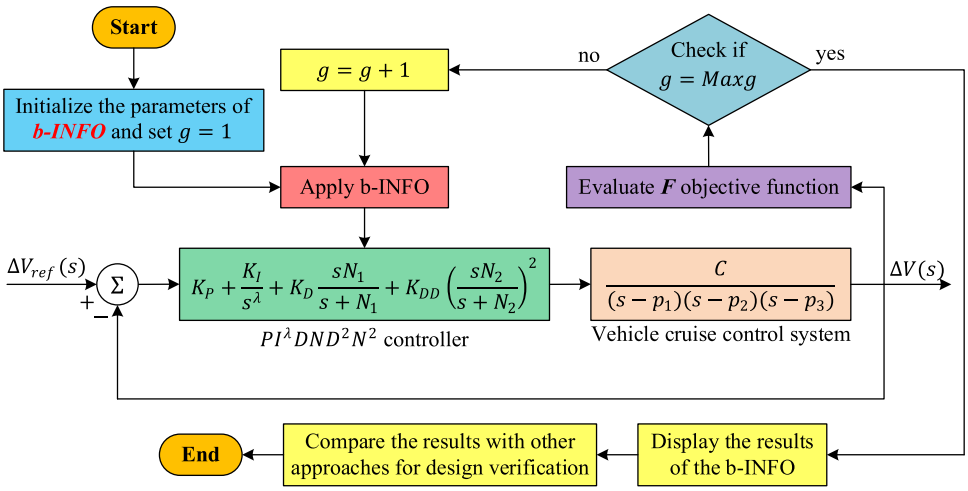


Fig. 7 Proposed $PI^{\lambda}DND^2N^2$ controller design procedure via b-INFO algorithm for vehicle cruise control system

Table 11 Parameter settings and time complexity of algorithms for vehicle cruise control system

Algorithm	Population size	Maximum iteration number	Values of other parameters	Time complexity (s)
b-INFO	30	50	$c = 2, d = 4$	37.81
INFO	30	50	$c = 2, d = 4$	35.93
MPA	30	50	$FADs = 0.2, P = 0.5$	47.76
GSA	30	50	$G_0 = 100, \alpha = 20$	44.57

Table 12 Statistical results of the F objective function

Algorithm	Mean	SD	Best	Worst
b-INFO	1.2565E−01	1.8125E−03	1.2303E−01	1.3053E−01
INFO	1.4239E−01	2.4901E−03	1.3889E−01	1.4710E−01
MPA	1.5624E−01	4.0594E−03	1.5072E−01	1.6896E−01
GSA	1.5590E−01	3.2229E−03	1.5126E−01	1.6321E−01

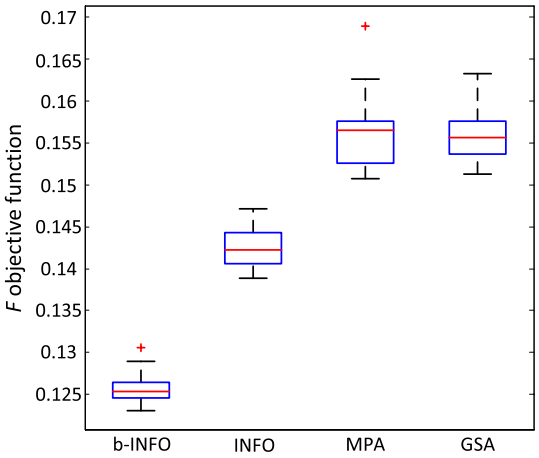


Fig. 8 Comparative boxplot analysis

complexity than all other algorithms. On the other hand, the proposed b-INFO algorithm has a slightly higher time complexity than the original form of INFO algorithm which is expected due to integration of EOBL and PS mechanisms. As mentioned earlier, the proposed b-INFO algorithm reaches significant solution quality at the expense of this slight increase in time complexity. However, it still occupies the second place in terms of less time complexity which the most convenient algorithm for the vehicle cruise control system.

The comparative statistical results obtained from the F objective function are provided numerically in Table 12. As can be seen from the latter table, the proposed b-INFO algorithm reaches the best statistical metrics for the employed objective function making it the most suitable approach for vehicle cruise control system.

Figure 8 presents the results of a boxplot analysis that highlights the superior performance of the proposed b-INFO algorithm. The plot shows that the proposed algorithm

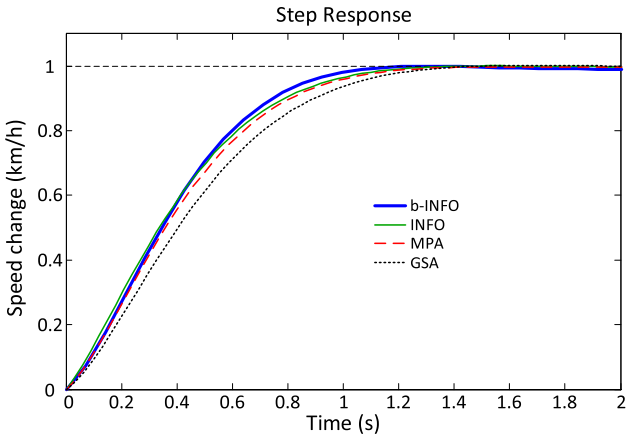


Fig. 9 Step responses of the system

outperforms the other algorithms by achieving the minimum value in the objective function. Moreover, the worst result obtained by the proposed b-INFO algorithm is still better than the best results obtained by the other algorithms, indicating the robustness and stability of the proposed algorithm.

The obtained $PI^{\lambda}DND^2N^2$ controller parameters (K_P, K_I, K_D, K_{DD}, λ, N_1 and N_2) for the best runs of the algorithms are presented in Table 13. Those values were used to perform the analysis presented in the following subsections for the respective algorithms-based controllers employed in a vehicle cruise control system.

7.3 Time Response Analysis

In this study, the time domain analysis was performed by considering the speed change step responses as demonstrated in Fig. 9. As can be observed, the proposed b-INFO algorithm is able to reach smoother response with no overshoot, less rise and settling times making it the most convenient approach amongst the other algorithms.

Table 14 presents a numerical comparison of the overshoot, rise time, settling time, and peak time of the proposed b-INFO algorithm-based $PI^{\lambda}DND^2N^2$ controller for the vehicle cruise control system with other algorithms. The results confirm the superior time response profile of the proposed controller, as it achieves lower values for rise time, settling time, and peak time while completely eliminating overshoot. This is consistent with the illustrative performance demonstrated in Fig. 9.

Table 13 Optimized parameters of $PI^{\lambda}DND^2N^2$ controller

Algorithm	K_P	K_I	K_D	K_{DD}	λ	N_1	N_2
b-INFO	5.2719	0.2469	5.9419	0.3173	0.9226	697.9591	508.6780
INFO	5.4360	0.1869	5.7632	0.4783	0.9690	449.6332	824.9288
MPA	4.9630	0.3216	5.5254	0.3494	1.0883	615.4430	664.6950
GSA	4.7132	0.1261	4.7422	0.2695	1.1326	842.1974	338.7143

Table 14 Comparison of transient response specifications

Algorithm	Overshoot (%)	Rise time (s)	Settling time (s)	Peak time (s)
b-INFO	0	0.6549	0.9893	1.2789
INFO	0.1051	0.7118	1.0875	1.5445
MPA	0.4866	0.7190	1.1204	3.0387
GSA	0.6066	0.7807	1.1815	1.6953

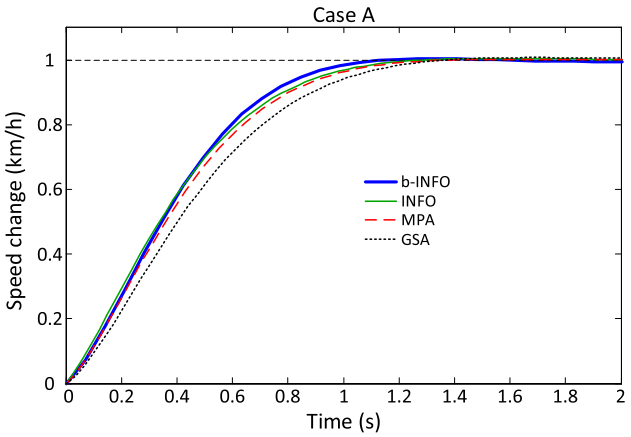


Fig. 10 Step responses of the system for $v_0 = 20\,\text{km/h}$

7.4 Robustness Analysis Under Different Operating Speeds

In this study, an operating speed of 30 km/h was initially considered for the analyses. In this section, the performance of the proposed approach is further evaluated by considering the robustness of the proposed b-INFO algorithm based $PI^{\lambda}DND^2N^2$ controller for vehicle cruise control system by separately considering different operating speeds. In this regard, operating speeds of 20 km/h (Case A) and 40 km/h (case B) were separately considered. Figure 10 illustrates the step response of the system for Case A while Fig. 11 shows for Case B. As can be observed from those figures, the proposed b-INFO algorithm demonstrates an overall better characteristic.

In addition, comparative numerical values for Case A and B are also provided in Table 15. As presented in this table, the proposed b-INFO algorithm achieves the lowest values for the overshoot, rise time, settling time and peak time for Case A demonstrating greater robustness. In case of Case B, all algorithms were able to reach no overshoot, however, the proposed b-INFO algorithm was also able to reach the shortest rise and settling time values confirming the excellent robustness of the proposed approach for different operating speeds.

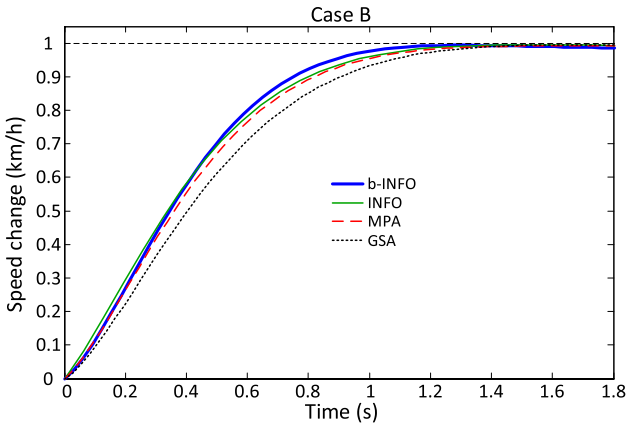


Fig. 11 Step responses of the system for $v_0 = 40\,\text{km/h}$

7.5 Comparison with the Most Recent Algorithms

Comparisons using the most recent reported methods of genetic algorithm (GA) based PID controller [4], ant lion optimizer (ALO) based PID controller [5], atom search optimization (ASO) algorithm based PID controller [18], arithmetic optimization algorithm (AOA) based PID controller [20], slime mould algorithm (SMA) based PID controller [20], Lévy flight distribution (LFD) algorithm based PID controller [20], manta ray foraging optimization (MRFO) based PID controller [20] and hunger games search (HGS) based PID controller [20] along with Harris hawks optimization (HHO) based PID and FOPID controllers [22] were employed, as well in order to provide an indication from a wider perspective.

Table 16 showcases the adopted parameters for the algorithms evaluated in this study, alongside their respective time complexity analyses. The numerical results presented in this table indicate that the proposed b-INFO algorithm-based $PI^{\lambda}DND^2N^2$ controller exhibits the lowest time complexity, highlighting its superior efficiency over the most recently reported approaches in terms of run time. Additionally, a comparison of the time domain performances of the different algorithms is illustrated in Fig. 12. The depicted figure demonstrates the exceptional effectiveness of the proposed b-INFO algorithm-based $PI^{\lambda}DND^2N^2$ controller among the most recently reported ones, achieving no overshoot along with minimum rise, settling, and peak times.

8 Conclusion

This paper presents a breakthrough in the field of vehicle cruise control systems by introducing a novel control approach that promises to revolutionize the industry. The proposed $PI^{\lambda}DND^2N^2$ controller, a first-of-its-kind in the

Table 15 Comparison of transient response specifications under different operating speeds

Case	Algorithm	Overshoot (%)	Rise time (s)	Settling time (s)	Peak time (s)
Case A ($v_0 = 20$ km/h)	b-INFO	0.5453	0.6480	0.9647	1.3384
	INFO	0.6914	0.7029	1.0522	1.5485
	MPA	1.0039	0.7112	1.0852	3.0464
	GSA	0.8915	0.7780	1.1685	1.6937
Case B ($v_0 = 40$ km/h)	b-INFO	0	0.6587	1.0208	16.6513
	INFO	0	0.7219	1.1312	33.4211
	MPA	0	0.7319	1.1925	3.0310
	GSA	0	0.8068	1.2934	1.6698

Table 16 Different reported methods along with their respective parameter values and the time complexity

Method no	Control method	Population size	Maximum iteration number	Values of other parameters	Time complexity (s)
1	GA-based PID [4]	40	25	$crossover = 0.8$, $mutation = 0.125$	NA
2	ALO-based PID [5]	10	150	$w \in [2, 6]$	NA
3	ASO-based PID [18]	50	100	$\alpha = 50$, $\beta = 0.2$	NA
4	AOA-based PID [20]	30	50	$\alpha = 5$, $\mu = 0.4975$	43.72
5	SMA based PID [20]	30	50	$z = 0.03$	50.94
6	LFD-based PID [20]	30	50	$Threshold = 2$, $C_{sv} = 0.5$, $\beta = 1.5$, $\alpha_1 = 10$, $\alpha_2 = 0.00005$, $\alpha_3 = 0.005$, $\partial_1 = 0.9$,$\partial_2 = 0.1$	181.61
7	MRFO-based PID [20]	30	50	$S = 2$	44.63
8	HGS-based PID [20]	30	50	$l = 0.03$, $LH = 100$	62.75
9	HHO-based PID [22]	30	50	$\beta = 1.5$, $E_0 \in [-1, 1]$	NA
10	HHO-based FOPID [22]	30	50	$\beta = 1.5$, $E_0 \in [-1, 1]$	NA
11	b-INFO-based $PI^{\lambda}DND^2N^2$ (proposed)	30	50	$c = 2$, $d = 4$	37.81

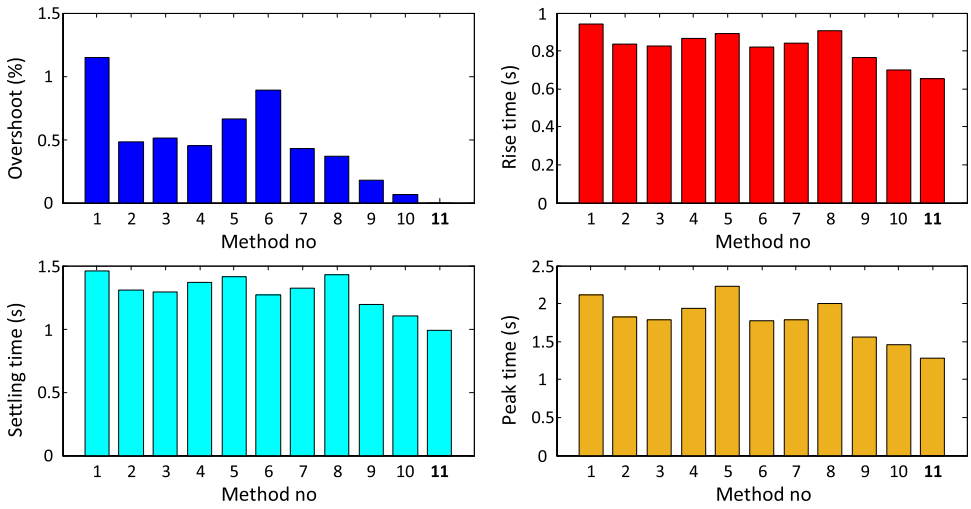


Fig. 12 Percent overshoot, rise time, settling time and peak time for different approaches

literature, has demonstrated outstanding effectiveness in controlling vehicle speed. To optimize the controller's parameters, the paper also introduces a cutting-edge metaheuristic algorithm called b-INFO, a boosted version of the INFO algorithm, leveraging the EOBL and PS mechanisms. The proposed b-INFO algorithm has been rigorously tested and validated through unimodal, multimodal, and fixed-dimensional multimodal benchmark functions, exhibiting exceptional performance. Furthermore, to attain the optimal parameters of the $PI^{\lambda}DND^2N^2$ controller, a well-designed objective function has been employed, leading to a highly efficient and robust method for controlling vehicle cruise control systems. Comparative analysis with other state-of-the-art algorithms, including INFO, MPA, and GSA algorithms, has demonstrated the superiority of the proposed b-INFO algorithm-based $PI^{\lambda}DND^2N^2$ the controller in controlling vehicle speed. The paper also compares the proposed method with the most recently reported approaches, demonstrating the remarkable capability of the proposed b-INFO based $PI^{\lambda}DND^2N^2$ controller to achieve unparalleled performance. In summary, this paper's innovative contribution has opened up new avenues for designing highly effective and efficient vehicle cruise control systems control approaches.

Authors Contributions All authors contributed equally to this paper.

Funding Open access funding provided by Linköping University. Authors have received no funding.

Data and Material Availability Data is available based on reasonable request.

Declarations

Conflict of interest The authors declare no conflict of interest.

Open Access This article is licensed under a Creative Commons Attribution 4.0 International License, which permits use, sharing, adaptation, distribution and reproduction in any medium or format, as long as you give appropriate credit to the original author(s) and the source, provide a link to the Creative Commons licence, and indicate if changes were made. The images or other third party material in this article are included in the article's Creative Commons licence, unless indicated otherwise in a credit line to the material. If material is not included in the article's Creative Commons licence and your intended use is not permitted by statutory regulation or exceeds the permitted use, you will need to obtain permission directly from the copyright holder. To view a copy of this licence, visit http://creativecommons.org/licenses/by/4.0/.

References

1. Pradhan, R., Majhi, S.K., Pradhan, J.K., Pati, B.B.: Performance evaluation of PID controller for an automobile cruise control system using ant lion optimizer. Eng. J. **21**, 347–361 (2017). https://doi.org/10.4186/ej.2017.21.5.347
2. Gulzar, M.M., Sharif, B., Sibtain, D., Akbar, L., Akhtar, A.: Modelling and controller design of automotive cruise control system using hybrid model predictive controller. In: 2019 15th International Conference on Emerging Technologies (ICET), pp. 1–5 (2019)
3. Blondin, M.J., Trovão, J.P.: Soft-computing techniques for cruise controller tuning for an off-road electric vehicle. IET Electr. Syst. Transp. **9**, 196–205 (2019). https://doi.org/10.1049/iet-est.2019.0008
4. Rout, M.K., Sain, D., Swain, S.K., Mishra, S.K.: PID controller design for cruise control system using genetic algorithm. In: 2016 International Conference on Electrical, Electronics, and Optimization Techniques (ICEEOT), pp. 4170–4174 (2016)
5. Pradhan, R., Majhi, S.K., Pradhan, J.K., Pati, B.B.: Antlion optimizer tuned PID controller based on Bode ideal transfer function for automobile cruise control system. J. Ind. Inf. Integr. **9**, 45–52 (2018). https://doi.org/10.1016/j.jii.2018.01.002
6. Pradhan, R., Pati, B.B.: Optimal FOPID controller for an automobile cruise control system. In: 2018 International Conference on Recent Innovations in Electrical, Electronics and Communication Engineering (ICRIEECE), pp. 1436–1440. IEEE, New York (2018)
7. Ekinci, S., Izci, D., Abualigah, L., Zitar, R.A.: A modified oppositional chaotic local search strategy based Aquila optimizer to design an effective controller for vehicle cruise control system. J. Bionic. Eng. (2023). https://doi.org/10.1007/s42235-023-00336-y
8. Onieva, E., Godoy, J., Villagrá, J., Milanés, V., Pérez, J.: On-line learning of a fuzzy controller for a precise vehicle cruise control system. Expert Syst. Appl. **40**, 1046–1053 (2013). https://doi.org/10.1016/j.eswa.2012.08.036
9. Huang, J., Chen, Y., Peng, X., Hu, L., Cao, D.: Study on the driving style adaptive vehicle longitudinal control strategy. IEEE/CAA J. Autom. Sin. **7**, 1107–1115 (2020). https://doi.org/10.1109/JAS.2020.1003261
10. Wu, W., Zou, D., Ou, J., Hu, L.: Adaptive cruise control strategy design with optimized active braking control algorithm. Math. Probl. Eng. **2020**, 1–10 (2020). https://doi.org/10.1155/2020/8382734
11. Moschos, I., Parisses, C.: A novel optimal PIλDND2N2 controller using coyote optimization algorithm for an AVR system. Eng. Sci. Technol. Int. J. **26**, 100991 (2022). https://doi.org/10.1016/j.jestch.2021.04.010
12. Agrawal, K., Negi, R., Singh, N.: Dynamically tuned PIDD2 controller for single-link flexible manipulator. Presented at the (2020)
13. Izci, D., Ekinci, S., Demiroren, A., Hedley, J.: HHO algorithm based PID controller design for aircraft pitch angle control system. In: 2020 International Congress on Human-Computer Interaction, Optimization and Robotic Applications (HORA), pp. 1–6. IEEE, New York (2020)
14. Ekinci, S., Izci, D., Hekimoglu, B.: Henry gas solubility optimization algorithm based FOPID controller design for automatic voltage regulator. In: 2020 International Conference on Electrical, Communication, and Computer Engineering (ICECCE), pp. 1–6. IEEE, New York (2020)
15. Izci, D., Ekinci, S., Zeynelgil, H.L., Hedley, J.: Performance evaluation of a novel improved slime mould algorithm for direct current motor and automatic voltage regulator systems. Trans. Inst. Meas. Control. **44**, 435–456 (2022). https://doi.org/10.1177/01423312211037967
16. Ekinci, S., Izci, D.: Enhanced reptile search algorithm with Lévy flight for vehicle cruise control system design. Evol Intell. (2022). https://doi.org/10.1007/s12065-022-00745-8
17. Bian, Q., Ma, J., Zhao, X., Wang, J., Meng, D.: Control parameter optimization for automobile cruise control system via improved

differential evolution algorithm. In: CICTP 2020, pp. 2236–2248. American Society of Civil Engineers, Reston, VA (2020)
18. Izci, D., Ekinci, S.: A novel hybrid ASO-NM algorithm and its application to automobile cruise control system. In: Mathur, G., Bundele, M., Mahendra, L., and Paprzycki, M. (eds.) 2nd International Conference on Artificial Intelligence: Advances and Applications, pp. 333–343. Springer, Singapore (2022)
19. Dawood, S.Y., et al.: Comparison of PID, GA and fuzzy logic controllers for cruise control system. Int. J. Comput. Dig. Syst. **7**, 311–319 (2018). https://doi.org/10.12785/ijcds/070505
20. Izci, D., Ekinci, S., Kayri, M., Eker, E.: A novel improved arithmetic optimization algorithm for optimal design of PID controlled and Bode's ideal transfer function based automobile cruise control system. Evol. Syst. **13**, 453–468 (2022). https://doi.org/10.1007/s12530-021-09402-4
21. Izci, D., Ekinci, S., Kayri, M., Eker, E.: A novel enhanced metaheuristic algorithm for automobile cruise control system. Electrica **21**, 283–297 (2021). https://doi.org/10.5152/electrica.2021.21016
22. Izci, D., Ekinci, S.: An efficient FOPID controller design for vehicle cruise control system using HHO algorithm. In: 2021 3rd International Congress on Human–Computer Interaction, Optimization and Robotic Applications (HORA), pp. 1–5. IEEE, New York (2021)
23. Ahmadianfar, I., Heidari, A.A., Noshadian, S., Chen, H., Gandomi, A.H.: INFO: an efficient optimization algorithm based on weighted mean of vectors. Expert Syst Appl. **195**, 116516 (2022). https://doi.org/10.1016/j.eswa.2022.116516
24. Sihwail, R., Omar, K., Ariffin, K.A.Z., Tubishat, M.: Improved harris hawks optimization using elite opposition-based learning and novel search mechanism for feature selection. IEEE Access **8**, 121127–121145 (2020). https://doi.org/10.1109/ACCESS.2020.3006473
25. Torczon, V.: On the convergence of pattern search algorithms. SIAM J. Optim. **7**, 1–25 (1997). https://doi.org/10.1137/S1052623493250780
26. Faramarzi, A., Heidarinejad, M., Mirjalili, S., Gandomi, A.H.: Marine predators algorithm: a nature-inspired metaheuristic. Expert Syst. Appl. **152**, 113377 (2020). https://doi.org/10.1016/j.eswa.2020.113377
27. Rashedi, E., Nezamabadi-pour, H., Saryazdi, S.: GSA: a gravitational search algorithm. Inf. Sci. (NY) **179**, 2232–2248 (2009). https://doi.org/10.1016/j.ins.2009.03.004
28. Tizhoosh, H.R.: Opposition-based learning: a new scheme for machine intelligence. In: International Conference on Computational Intelligence for Modelling, Control and Automation and International Conference on Intelligent Agents, Web Technologies and Internet Commerce (CIMCA-IAWTIC'06), pp. 695–701. IEEE, New York (2005)
29. Izci, D., Ekinci, S., Eker, E., Kayri, M.: Augmented hunger games search algorithm using logarithmic spiral opposition-based learning for function optimization and controller design. J. King Saud Univ. Eng. Sci. (2022). https://doi.org/10.1016/j.jksues.2022.03.001
30. Izci, D., Ekinci, S., Eker, E., Kayri, M.: A novel modified opposition-based hunger games search algorithm to design fractional order proportional–integral–derivative controller for magnetic ball suspension system. Adv. Control Appl. **4**, 96 (2022). https://doi.org/10.1002/adc2.96
31. Khanduja, N., Bhushan, B.: Chaotic state of matter search with elite opposition based learning: a new hybrid metaheuristic algorithm. Optim. Control Appl. Methods (2021). https://doi.org/10.1002/oca.2810
32. Eslami, M., Neshat, M., Khalid, S.A.: A novel hybrid sine cosine algorithm and pattern search for optimal coordination of power system damping controllers. Sustainability. **14**, 541 (2022). https://doi.org/10.3390/su14010541
33. Lewis, P.H., Houghton, Y.: Basic Control Systems Engineering. Prentice Hall, Upper Saddle River (1997)
34. Ekinci, S., Izci, D., Al Nasar, M.R., Abu Zitar, R., Abualigah, L.: Logarithmic spiral search based arithmetic optimization algorithm with selective mechanism and its application to functional electrical stimulation system control. Soft Comput. **26**, 12257–12269 (2022). https://doi.org/10.1007/s00500-022-07068-x
35. Izci, D., Ekinci, S., Zeynelgil, H.L., Hedley, J.: Fractional order PID design based on novel improved slime mould algorithm. Electric Power Components Syst. **49**, 901–918 (2021). https://doi.org/10.1080/15325008.2022.2049650
36. Izci, D., Ekinci, S.: A novel improved version of hunger games search algorithm for function optimization and efficient controller design of buck converter system. e-Prime Adv. Electr. Eng. Electron. Energy. **2**, 100039 (2022). https://doi.org/10.1016/j.prime.2022.100039
37. Raju, M., Saikia, L.C., Sinha, N.: Automatic generation control of a multi-area system using ant lion optimizer algorithm based PID plus second order derivative controller. Int. J. Electr. Power Energy Syst. **80**, 52–63 (2016). https://doi.org/10.1016/j.ijepes.2016.01.037
38. Jaradat, M.A., Sawaqed, L.S., Alzgool, M.M.: Optimization of PIDD2-FLC for blood glucose level using particle swarm optimization with linearly decreasing weight. Biomed Signal Process Control **59**, 101922 (2020). https://doi.org/10.1016/j.bspc.2020.101922
39. Tepljakov, A.: FOMCON: fractional-order modeling and control toolbox. In: Fractional-Order Modeling and Control of Dynamic Systems, pp. 107–129. Springer, London (2017)
40. Izci, D.: Design and application of an optimally tuned PID controller for DC motor speed regulation via a novel hybrid Lévy flight distribution and Nelder–Mead algorithm. Trans. Inst. Meas. Control **43**, 3195–3211 (2021). https://doi.org/10.1177/01423312211019633

Publisher's Note Springer Nature remains neutral with regard to jurisdictional claims in published maps and institutional affiliations.